

# New galaxy UV luminosity constraints on warm dark matter from JWST

BIN LIU<sup>1</sup>, HUANYUAN SHAN<sup>1,2,3</sup> AND JIAJUN ZHANG<sup>1, 2, 3</sup>

<sup>1</sup>*Shanghai Astronomical Observatory, Chinese Academy of Sciences, Nandan Road 80, Shanghai 200030, China*

<sup>2</sup>*School of Astronomy and Space Science, University of Chinese Academy of Sciences, Beijing 100049, China*

<sup>3</sup>*Key Laboratory of Radio Astronomy and Technology, Chinese Academy of Sciences, A20 Datun Road, Chaoyang District, Beijing, 100101, P. R. China*

## ABSTRACT

We exploit the recent *James Webb Space Telescope* (JWST) determination of galaxy UV luminosity functions over the redshift range  $z = 9 - 14.5$  to derive constraints on warm dark matter (WDM) models. The delayed structure formation in WDM universe makes high redshift observations to be a powerful probe to set limits on the particle mass  $m_x$  of WDM candidates. By integrating these observations with blank-field surveys conducted by *Hubble Space Telescope* (HST) at redshifts  $z = 4 - 8$ , we impose constraints on both astrophysical and WDM parameters simultaneously. We find a new limit of  $m_x \geq 3.2$  keV for the mass of thermal relic WDM particles at 95% confidence level. This bound is tighter than the most stringent result derived using HST data before. Future JWST observations could further reduce the observation uncertainties and improve this constraint.

*Keywords:* dark matter - galaxies: high-redshift

## 1. INTRODUCTION

Understanding the nature of dark matter remains one of the most important challenges in the field of cosmology. Despite dark matter makes up  $\sim 85\%$  of matter content in the universe, definitive detection of dark matter remains elusive. While the cold dark matter (CDM) cosmological model is notably consistent with most observational data, small scale challenges (see e.g. Bullock & Boylan-Kolchin 2017) also prompt exploration of dark matter models beyond standard CDM.

Many alternative candidates such as warm dark matter (WDM), fuzzy dark matter or

self-interacting dark matter (Bode et al. 2001; Hu et al. 2000; Spergel & Steinhardt 2000) have been proposed to give a better explanation of structure formation at small scales. These scenarios produce a suppression in the matter power spectrum and hold significant implications for various cosmological observations. Constraints on these non-standard dark matter models have been derived from various astrophysical probes, including the Lyman- $\alpha$  forest (Viel et al. 2013; Baur et al. 2016; Irsič et al. 2017; Garzilli et al. 2021; Villasenor et al. 2023),  $\gamma$ -ray burst (de Souza et al. 2013), strong gravitational lensing (Gilman et al. 2019, 2020; Shevchuk et al. 2023), Milky Way satellite galaxies (Kennedy et al. 2014; Nadler et al. 2021a,b; Newton et al. 2021), neu-

Corresponding author: Huanyuan Shan  
[hyshan@shao.ac.cn](mailto:hyshan@shao.ac.cn)

tral hydrogen 21cm signal (Chatterjee et al. 2019; Rudakovskyi et al. 2020) and high redshift galaxy number counts or luminosity functions (Pacucci et al. 2013; Schultz et al. 2014; Corasaniti et al. 2017; Gandolfi et al. 2022; Maio & Viel 2023).

The galaxy UV luminosity function (UVLF) is considered a potent tool for constraining warm dark matter models. In fact, these models yield an exponential suppression on small scale structures at early cosmic time. The detection of high redshift galaxies can capture this characteristic and establish stringent limits on WDM particle mass. During the *Hubble Space Telescope* (HST) era, UVLF observations have already reached to redshift  $z = 10$ , and tight lower boundaries have been obtained from these results (Menci et al. 2016a,b, 2017; Rudakovskyi et al. 2021). As anticipated by these studies, observations from the *James Webb Space Telescope* (JWST) will further enhance constraint power on the particle mass in WDM models.

The early data release of JWST has shown the detection of very distant galaxies up to  $z = 14 - 16$  and has reliably mapped UVLF at redshift  $z \geq 10$  (e.g. Castellano et al. 2022; Naidu et al. 2022; Finkelstein et al. 2023; Casey et al. 2023; Adams et al. 2023; Bouwens et al. 2023; Donnan et al. 2023; Harikane et al. 2023). These findings enable us to constrain the nature of dark matter based on the properties of the first generation galaxies in the Universe. Recently, Donnan et al. (2024) combined several major Cycle-1 JWST imaging programs to compile a large and deep sample. Taking the advantage of the larger region coverage, the accuracy of UVLF measurement is markedly improved. In this paper, we utilize the new UVLF measurements from JWST as well as the previous results from HST to perform new constraint on WDM models.

This paper is structured as follows. In Sec.2, we describe our UVLF model and data sets. In

Sec.3, we present the results derived from our analysis, followed by conclusions drawn in Sec.4.

Throughout this paper, we assume the fiducial model is a flat  $\Lambda$ CDM cosmology with  $H_0 = 67.4 \text{ km s}^{-1} \text{ Mpc}^{-1}$ ,  $\Omega_m = 0.315$ ,  $\Omega_b = 0.049$ ,  $\sigma_8 = 0.811$  and  $n_s = 0.965$ .

## 2. METHODOLOGY

The UVLF is defined as the number density of galaxies as a function of their UV magnitude. By connecting galaxy properties to dark matter halos, the UVLF can be written as:

$$\Phi_{\text{UV}} = \frac{dn_h}{dM_h} \times \frac{dM_h}{dM_{\text{UV}}} \quad (1)$$

with the first term  $\frac{dn_h}{dM_h}$  is the halo mass function, while the subsequent function  $\frac{dM_h}{dM_{\text{UV}}}$  establishes the connection between halo mass and galaxy luminosity.

To construct the theoretical UVLF, we should first know the dark matter halo mass function. The halo mass function characterizes the mass distribution of dark matter halos. In the case of CDM, the halo mass function is expressed as:

$$\frac{dn_h}{dM_h} = \bar{\rho}_m \frac{d \ln \sigma_{M_h}^{-1}}{dM_h} f(\sigma_{M_h}) \quad (2)$$

Here  $\bar{\rho}_m$  denotes the average comoving matter energy density, and  $\sigma_{M_h}$  is the root-mean-square of the density field smoothed over a mass scale  $M_h$ , typically computed using a top-hat window function and the linear power spectrum. The linear power spectrum can be calculated using publicly available codes CLASS(Blas et al. 2011) or CAMB (Lewis et al. 2000). The function  $f(\sigma_{M_h})$  is obtained analytically or measured from simulations. We adopt the Sheth-Tormen form (Sheth & Tormen 2002) in our models.

In the WDM scenarios, the halo mass function experiences suppression below a characteristic halo mass, which correlates with the mass of the WDM particle. This suppression can be fitted by a parameterized function:

$$n_{\text{WDM}}/n_{\text{CDM}} = \left(1 + (aM_{\text{hm}}/M_{\text{WDM}})^b\right)^c \quad (3)$$

where  $M_{\text{WDM}}$  is the halo mass of WDM halos,  $M_{\text{hm}}$  denotes the half model mass, which depends on the dark matter particle mass  $m_x$ , and  $a$ ,  $b$  and  $c$  are fitting parameters. We evaluate the fitting functions using the results reported in Stücker et al. (2022).

The function  $\frac{dM_h}{dM_{\text{UV}}}$  connects the halo mass with the galaxy luminosity. The UV luminosity of a galaxy is correlated with its star formation rate through (Madau & Dickinson 2014):

$$\text{SFR} = \mathcal{K}_{\text{UV}} \times L_{\text{UV}} \quad (4)$$

Assuming a Salpeter initial mass function (Salpeter 1955), the conversion factor is determined to be  $\mathcal{K}_{\text{UV}} = 1.15 \times 10^{-28}$ . On the other hand, we can also connect star formation rate with halo mass through the baryonic accretion rate:

$$\text{SFR} = f_* \times \dot{M}_b \quad (5)$$

Following (Sun & Furlanetto 2016), we adopt the baryonic accretion rate as:

$$\dot{M}_b \approx 3M_\odot/\text{yr} \left(\frac{M_h}{10^{10}M_\odot}\right)^\delta \left(\frac{1+z}{7}\right)^\eta \quad (6)$$

with  $\delta = 1.127$ ,  $\eta = 2.5$  and  $M_h$  representing the halo mass.  $f_*$  is the star formation efficiency (SFE), and we employ a double power law model:

$$f_* = \frac{2\epsilon_N}{\left(\frac{M_h}{M_c}\right)^\beta + \left(\frac{M_h}{M_c}\right)^\gamma} \quad (7)$$

where  $\epsilon_N$  is the amplitude of SFE, while  $\beta$  and  $\gamma$  regulate the slope of SFE at low and high masses, respectively.  $M_c$  determines the halo mass at which the SFE peaks.

Combining the above equations together, we can get the UVLF as a function of the WDM

model parameter as well as the astrophysical parameters. This function relates luminosity of a galaxy to a particular halo mass. Additionally, we also incorporate a Gaussian form stochasticity in the function, as demonstrated in other studies (e.g. Sabti et al. 2022):

$$P(M_{\text{UV}}) = \frac{1}{\sqrt{2\pi}\sigma_{M_{\text{UV}}}} \exp\left[-\frac{(M_{\text{UV}} - \langle M_{\text{UV}} \rangle)^2}{2\sigma_{M_{\text{UV}}}^2}\right] \quad (8)$$

where  $\langle M_{\text{UV}} \rangle$  is the average magnitude calculated from the one-to-one luminosity-halo relation described above, and  $\sigma_{M_{\text{UV}}}$  is the stochasticity parameter, which we treated as a free parameter in our fitting process. Taking stochasticity into consideration, the final luminosity function is:

$$\Phi_{\text{UV}}(z, M_{\text{UV}}, \boldsymbol{\theta}) = \frac{1}{\Delta M_{\text{UV}}} \int_0^\infty dM_h \left[ \frac{dn_{\text{WDM}}}{dM_h}(z, M_h, \boldsymbol{\theta}) \times \int_{M_{\text{UV},1}}^{M_{\text{UV},2}} dM'_{\text{UV}} P(M'_{\text{UV}}, z, M_h, \boldsymbol{\theta}) \right] \quad (9)$$

with  $\boldsymbol{\theta}$  represents the parameter set in our model,  $\boldsymbol{\theta} = \{\epsilon_N, \beta, \gamma, M_c, \sigma_{M_{\text{UV}}}, m_x\}$ .

To estimate these parameters, we perform the analysis with Markov chain Monte-Carlo (MCMC) sampling via Python package `emcee` (Foreman-Mackey et al. 2013). We use a modified version of `GALLUMI` (Sabti et al. 2022) likelihood:

$$-2 \ln \mathcal{L} = \sum_{M_{\text{UV}}, z} \left( \frac{\Phi_{\text{model}}(z, M_{\text{UV}}, \boldsymbol{\theta}) - \Phi_{\text{data}}}{\sigma_{\Phi}^{\text{data}}} \right)^2 \quad (10)$$

where  $\Phi_{\text{model}}(z, M_{\text{UV}}, \boldsymbol{\theta})$  is the theoretical luminosity function at each magnitude bin and redshift computed above, and  $\Phi_{\text{data}}$  and  $\sigma_{\Phi}^{\text{data}}$  are the measured UVLF and errors, respectively. The priors for our parameters are listed in Table 1. It's worth noting that we use  $1/m_x$  instead of  $m_x$  in the fitting. This choice is made

because the larger values of  $m_x$  tend to converge to CDM model results and there are no reliable upper limits.

Parameter	Prior Value	Units	Prior form
$\epsilon_N$	$10^{-3} - 1.0$	-	flat log
$\beta$	$-3.0 - 0.0$	-	flat linear
$\gamma$	$0.0 - 3.0$	-	flat linear
$M_c$	$10^7 - 10^{15}$	$M_\odot$	flat log
$\sigma_{\text{UV}}$	$10^{-3} - 3.0$	-	flat linear
$1/m_x$	$0 - 1$	$\text{keV}^{-1}$	flat linear

**Table 1.** The parameters and their priors used in our analysis.

The dataset encompasses both HST and JWST observations spanning the redshift range  $z = 4$  to  $z = 14.5$ . JWST has extended the detection of UVLF to higher redshifts. Recently, [Donnan et al. \(2024\)](#) combined several major Cycle-1 JWST imaging programs to produce a new determination. This determination yields a UVLF measurement over an area of  $\sim 370$  sq. arcmin across the redshift range  $z = 9 - 14.5$ . Combining these new JWST results with previous HST observations ([Bouwens et al. 2021](#)) at redshift  $z = 4 - 8$ , we create a comprehensive sample spanning the widest redshift range for our analysis. The final sample is shown in Figure 1. Additionally, We account the effects of dust extinction and apply a correction to the lower redshift and brighter magnitude ends of the data. Assuming the IBX –  $\beta$  relation, the extinction parameter is then calculated as:

$$\langle A_{\text{UV}} \rangle = C_0 + 0.2 \ln(10) \sigma_\beta^2 C_1^2 + C_1 \langle \beta_{\text{dust}} \rangle \quad (11)$$

and we adopt the values of the parameters  $C_0$ ,  $C_1$ ,  $\sigma_\beta$  and  $\beta_{\text{dust}}$  following [Sabti et al. \(2022\)](#).

### 3. RESULTS

Figure 2 presents the MCMC results for all parameters within our model. The astrophysical

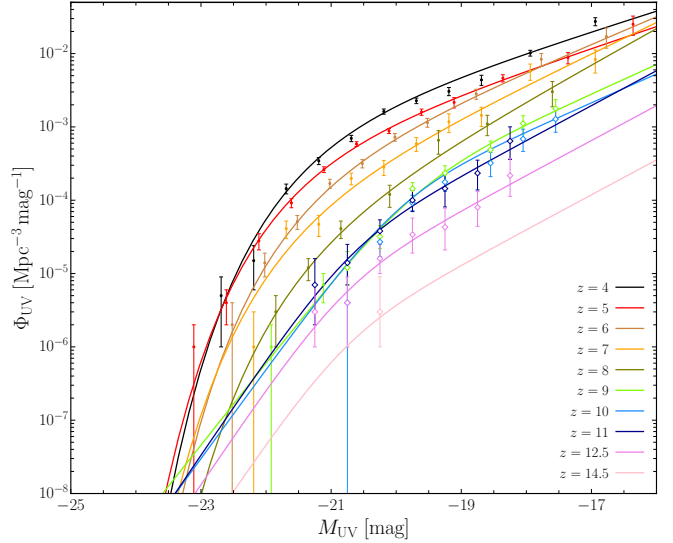


**Figure 1.** The UVLF data obtained from HST and JWST. HST data are marked with solid circles, while JWST data are marked with open diamonds. Solid lines represent the Schechter or Double power law fits to these data.

parameters are consistent with previous studies (e.g. [Moster et al. 2018; Harikane et al. 2022](#)). Here we seldom pay attention on these parameters and only focus on the dark matter particle mass  $m_x$ . It is shown that current data can not rule out WDM models or favor a specific WDM particle mass. Typically, a lower limit is given by UVLF or other probes. The bottom right panel of Figure 2 shows the marginalized 1D posteriors of  $m_x$ . As illustrated in this figure, the 95% credible limit reaches to  $m_x \geq 3.2$  keV. This result suggests that JWST observations can further enhance the constraint power on WDM, aligning with earlier forecast made by [Rudakovskiy et al. \(2021\)](#) based on simulated JWST results ([Park et al. 2020](#)). Our lower bound is even tighter than their prediction due to the broader redshift coverage.

Our result update the tightest constraint derived from UVLF method. Previous studies have obtained several limits by comparing the cumulative galaxy number or fitting the analytic models to UVLF observations. The tightest result was obtained by [Menci et al. \(2016a\)](#)

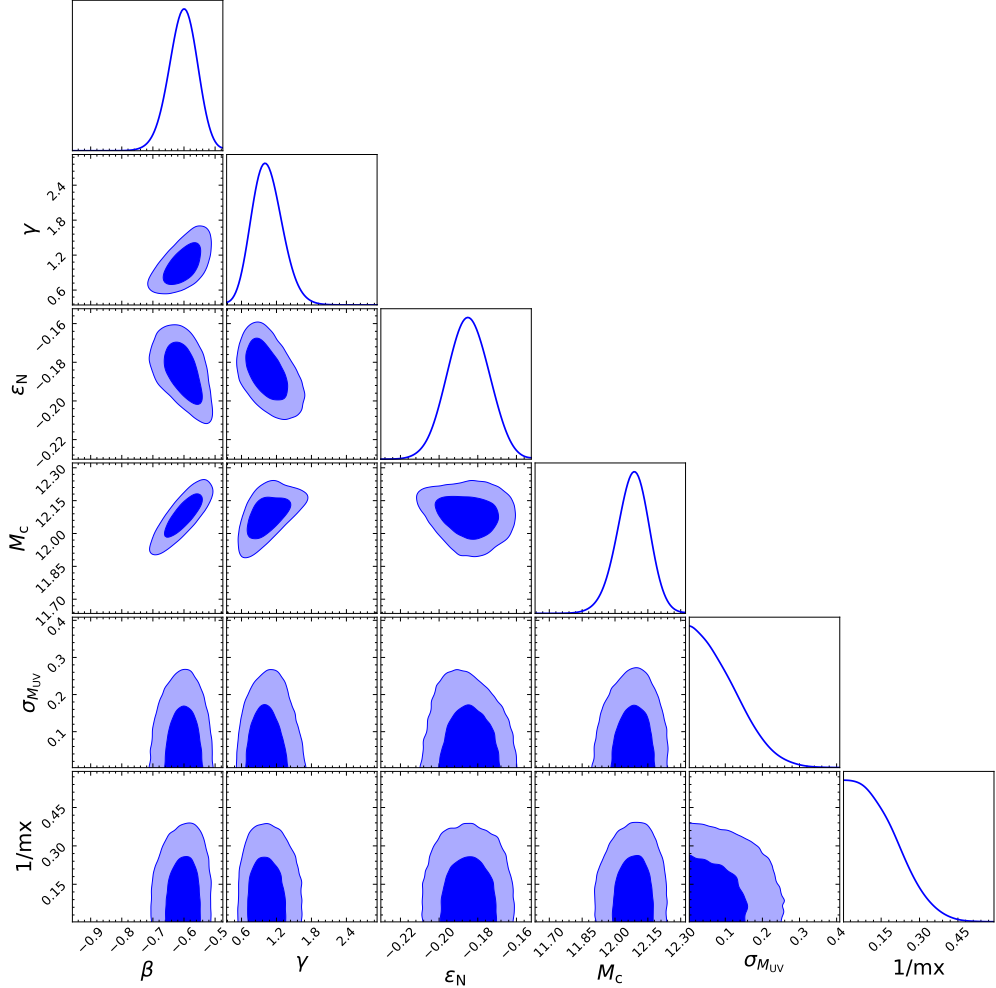


**Figure 2.** Posterior distributions of the astrophysical parameters and the inverse of dark matter particle mass. The contours show 68% and 95% confidence intervals. The lower bound of WDM particle mass parameter reaches to  $m_x \geq 3.2$  keV at 95% confidence interval.

using the galaxy number counts. Compared to their findings, we derive a tighter constraint with the inclusion of high-redshift JWST data. Figure 3 shows our new constraint compared with several tight results derived from other UVLF research (Menci et al. 2016a; Corasaniti et al. 2017; Rudakovskiy et al. 2021; Maio & Viel 2023). Furthermore, even tighter limits obtained from the analysis of strongly lensed quasars (Gilman et al. 2020; Hsueh et al. 2020), Milky Way Satellites (Nadler et al. 2021b), Lyman- $\alpha$  forest (Baur et al. 2016; Iršič et al. 2017) or a combination of these probes (Enzi et al. 2021; Nadler et al. 2021a) are also illustrated. Although the results derived from

UVLF are not the most stringent constraints, these results provide comprehensive exploration at high redshift. Meanwhile, robust limits have not been established, conservative estimations of these approaches lead to weaker lower bounds (Garzilli et al. 2021; Newton et al. 2021), our constraint can serve as cross validation in testing the nature of dark matter.

#### 4. CONCLUSION

Current and upcoming JWST surveys can provide improved measurements on the abundance and brightness of galaxies at early universe. This will enable us to detect the nature of dark matter by making use of the UVLF of

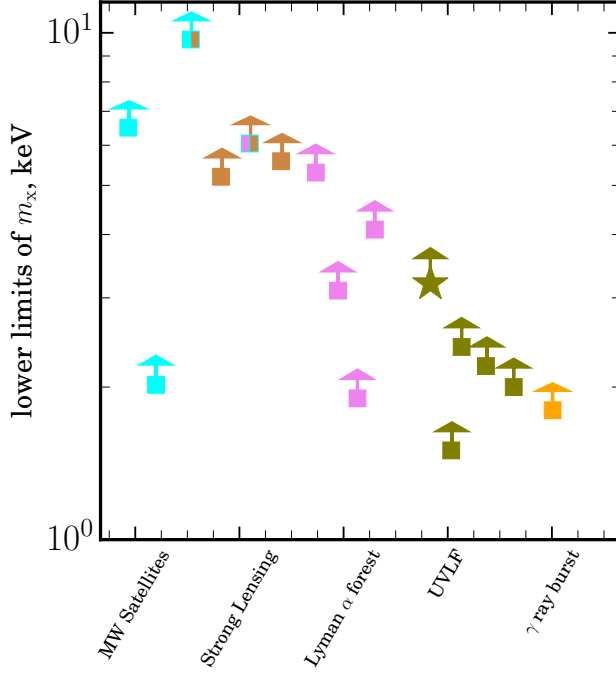


**Figure 3.** Lower limits of  $m_x$  derived from different probes: Milky Way satellites (cyan, Newton et al. 2021; Nadler et al. 2021b), strong gravitational lensing (peru, Hsueh et al. 2020; Gilman et al. 2020), Lyman  $\alpha$  forest (violet, Baur et al. 2016; Iršič et al. 2017; Garzilli et al. 2021; Vilasenor et al. 2023), UVLF (olive, Menci et al. 2016a; Corasaniti et al. 2017; Rudakovskiy et al. 2021; Maio & Viel 2023),  $\gamma$  ray burst (orange, de Souza et al. 2013) or joint analysis (mixed color, Enzi et al. 2021; Nadler et al. 2021a). Star symbol denotes the result derived from this work.

galaxies. In this work, we have compiled the most extensive determination of UVLF from JWST, along with previous blank-field surveys conducted by HST to make a widest UVLF sample spanning from redshift  $z = 4$  to  $z = 14.5$ . We then perform astrophysical constraints on WDM cosmologies with this sample.

Employing a double power law astrophysical model, we simultaneously fit the astrophysical and WDM parameters. Based on current observations, we find the 95% credible limit of the lower boundary is  $m_x \geq 3.2$  keV for thermal

relic WDM particles. This is the most stringent constraint derived from UVLF and corroborates previous forecast that early JWST results would imply a WDM particle mass to  $m_x > 2.5$  keV.

The constraint could be further improved in the future by extending the current detection of faint objects to cover a larger area or to deeper magnitude limits. As an example, assuming that the current deepest region ( $\sim 30$  AB mag) maintains the same area coverage ( $\sim 370$  sq. arcmin), the measurement will improve the lower bound to  $m_x \geq 4.3$  keV. Future programs could carry out the necessary observations to validate this calculation. Additionally, JWST will not only improve the data quality for bright galaxies, the detection limit is also extended. With the assistance of cluster lensing magnification, the depth of observations can reach to  $\sim 31 - 34$  mag. Precise and deep observation will yield stronger constraints which would comparable to the results inferred from lensed quasars, albeit long observational time is required.

## 5. ACKNOWLEDGEMENTS

We acknowledge the support by National Key R&D Program of China No. 2022YFF0503403, No.2022YFF0504300 and the Ministry of Science and Technology of China (grant Nos. 2020SKA0110100). This work is supported by China Manned Space Project (No. CMS-CSST-2021-A01, CMS-CSST-2021-A04, CMS-CSST-2021-A07, CMS-CSST-2023-A03). BL acknowledges the Shanghai Post-doctoral Excellence Program under Grant No. 2022671. HYS acknowledges the support from NSFC of China under grant 11973070, Key Research Program of Frontier Sciences, CAS, Grant No. ZDBS-LY-7013 and Program of Shanghai Academic/Technology Research Leader. JZ acknowledges the support from the China Manned Space Project with no. CMS-CSST-2021-A03.

## REFERENCES

- Adams, N. J., Conselice, C. J., Austin, D., et al. 2023, arXiv e-prints, arXiv:2304.13721, doi: [10.48550/arXiv.2304.13721](https://doi.org/10.48550/arXiv.2304.13721)
- Baur, J., Palanque-Delabrouille, N., Yèche, C., Magneville, C., & Viel, M. 2016, *JCAP*, 2016, 012, doi: [10.1088/1475-7516/2016/08/012](https://doi.org/10.1088/1475-7516/2016/08/012)
- Blas, D., Lesgourgues, J., & Tram, T. 2011, *JCAP*, 2011, 034, doi: [10.1088/1475-7516/2011/07/034](https://doi.org/10.1088/1475-7516/2011/07/034)
- Bode, P., Ostriker, J. P., & Turok, N. 2001, *ApJ*, 556, 93, doi: [10.1086/321541](https://doi.org/10.1086/321541)
- Bouwens, R. J., Oesch, P. A., Stefanon, M., et al. 2021, *AJ*, 162, 47, doi: [10.3847/1538-3881/abf83e](https://doi.org/10.3847/1538-3881/abf83e)
- Bouwens, R. J., Stefanon, M., Brammer, G., et al. 2023, *MNRAS*, 523, 1036, doi: [10.1093/mnras/stad1145](https://doi.org/10.1093/mnras/stad1145)
- Bullock, J. S., & Boylan-Kolchin, M. 2017, *ARA&A*, 55, 343, doi: [10.1146/annurev-astro-091916-055313](https://doi.org/10.1146/annurev-astro-091916-055313)
- Casey, C. M., Akins, H. B., Shuntov, M., et al. 2023, arXiv e-prints, arXiv:2308.10932, doi: [10.48550/arXiv.2308.10932](https://doi.org/10.48550/arXiv.2308.10932)
- Castellano, M., Fontana, A., Treu, T., et al. 2022, *ApJL*, 938, L15, doi: [10.3847/2041-8213/ac94d0](https://doi.org/10.3847/2041-8213/ac94d0)
- Chatterjee, A., Dayal, P., Choudhury, T. R., & Hutter, A. 2019, *MNRAS*, 487, 3560, doi: [10.1093/mnras/stz1444](https://doi.org/10.1093/mnras/stz1444)
- Corasaniti, P. S., Agarwal, S., Marsh, D. J. E., & Das, S. 2017, *PhRvD*, 95, 083512, doi: [10.1103/PhysRevD.95.083512](https://doi.org/10.1103/PhysRevD.95.083512)
- de Souza, R. S., Mesinger, A., Ferrara, A., et al. 2013, *MNRAS*, 432, 3218, doi: [10.1093/mnras/stt674](https://doi.org/10.1093/mnras/stt674)
- Donnan, C. T., McLeod, D. J., Dunlop, J. S., et al. 2023, *MNRAS*, 518, 6011, doi: [10.1093/mnras/stac3472](https://doi.org/10.1093/mnras/stac3472)
- Donnan, C. T., McLure, R. J., Dunlop, J. S., et al. 2024, arXiv e-prints, arXiv:2403.03171, doi: [10.48550/arXiv.2403.03171](https://doi.org/10.48550/arXiv.2403.03171)
- Enzi, W., Murgia, R., Newton, O., et al. 2021, *MNRAS*, 506, 5848, doi: [10.1093/mnras/stab1960](https://doi.org/10.1093/mnras/stab1960)
- Finkelstein, S. L., Bagley, M. B., Ferguson, H. C., et al. 2023, *ApJL*, 946, L13, doi: [10.3847/2041-8213/acad4](https://doi.org/10.3847/2041-8213/acad4)
- Foreman-Mackey, D., Hogg, D. W., Lang, D., & Goodman, J. 2013, *PASP*, 125, 306, doi: [10.1086/670067](https://doi.org/10.1086/670067)
- Gandolfi, G., Lapi, A., Ronconi, T., & Danese, L. 2022, *Universe*, 8, 589, doi: [10.3390/universe8110589](https://doi.org/10.3390/universe8110589)
- Garzilli, A., Magalich, A., Ruchayskiy, O., & Boyarsky, A. 2021, *MNRAS*, 502, 2356, doi: [10.1093/mnras/stab192](https://doi.org/10.1093/mnras/stab192)
- Gilman, D., Birrer, S., Nierenberg, A., et al. 2020, *MNRAS*, 491, 6077, doi: [10.1093/mnras/stz3480](https://doi.org/10.1093/mnras/stz3480)
- Gilman, D., Birrer, S., Treu, T., Nierenberg, A., & Benson, A. 2019, *MNRAS*, 487, 5721, doi: [10.1093/mnras/stz1593](https://doi.org/10.1093/mnras/stz1593)
- Harikane, Y., Nakajima, K., Ouchi, M., et al. 2023, arXiv e-prints, arXiv:2304.06658, doi: [10.48550/arXiv.2304.06658](https://doi.org/10.48550/arXiv.2304.06658)
- Harikane, Y., Ono, Y., Ouchi, M., et al. 2022, *ApJS*, 259, 20, doi: [10.3847/1538-4365/ac3dfc](https://doi.org/10.3847/1538-4365/ac3dfc)
- Hsueh, J. W., Enzi, W., Vegetti, S., et al. 2020, *MNRAS*, 492, 3047, doi: [10.1093/mnras/stz3177](https://doi.org/10.1093/mnras/stz3177)
- Hu, W., Barkana, R., & Gruzinov, A. 2000, *PhRvL*, 85, 1158, doi: [10.1103/PhysRevLett.85.1158](https://doi.org/10.1103/PhysRevLett.85.1158)
- Iršič, V., Viel, M., Haehnelt, M. G., et al. 2017, *Phys. Rev. D*, 96, 023522, doi: [10.1103/PhysRevD.96.023522](https://doi.org/10.1103/PhysRevD.96.023522)
- Kennedy, R., Frenk, C., Cole, S., & Benson, A. 2014, *MNRAS*, 442, 2487, doi: [10.1093/mnras/stu719](https://doi.org/10.1093/mnras/stu719)
- Lewis, A., Challinor, A., & Lasenby, A. 2000, *ApJ*, 538, 473, doi: [10.1086/309179](https://doi.org/10.1086/309179)
- Madau, P., & Dickinson, M. 2014, *ARA&A*, 52, 415, doi: [10.1146/annurev-astro-081811-125615](https://doi.org/10.1146/annurev-astro-081811-125615)
- Maio, U., & Viel, M. 2023, *A&A*, 672, A71, doi: [10.1051/0004-6361/202345851](https://doi.org/10.1051/0004-6361/202345851)
- Menci, N., Grazian, A., Castellano, M., & Sanchez, N. G. 2016a, *ApJL*, 825, L1, doi: [10.3847/2041-8205/825/1/L1](https://doi.org/10.3847/2041-8205/825/1/L1)
- Menci, N., Merle, A., Totzauer, M., et al. 2017, *ApJ*, 836, 61, doi: [10.3847/1538-4357/836/1/61](https://doi.org/10.3847/1538-4357/836/1/61)
- Menci, N., Sanchez, N. G., Castellano, M., & Grazian, A. 2016b, *ApJ*, 818, 90, doi: [10.3847/0004-637X/818/1/90](https://doi.org/10.3847/0004-637X/818/1/90)
- Moster, B. P., Naab, T., & White, S. D. M. 2018, *MNRAS*, 477, 1822, doi: [10.1093/mnras/sty655](https://doi.org/10.1093/mnras/sty655)
- Nadler, E. O., Birrer, S., Gilman, D., et al. 2021a, *ApJ*, 917, 7, doi: [10.3847/1538-4357/abf9a3](https://doi.org/10.3847/1538-4357/abf9a3)
- Nadler, E. O., Drlica-Wagner, A., Bechtol, K., et al. 2021b, *PhRvL*, 126, 091101, doi: [10.1103/PhysRevLett.126.091101](https://doi.org/10.1103/PhysRevLett.126.091101)

- Naidu, R. P., Oesch, P. A., van Dokkum, P., et al. 2022, ApJL, 940, L14, doi: [10.3847/2041-8213/ac9b22](https://doi.org/10.3847/2041-8213/ac9b22)
- Newton, O., Leo, M., Cautun, M., et al. 2021, JCAP, 2021, 062, doi: [10.1088/1475-7516/2021/08/062](https://doi.org/10.1088/1475-7516/2021/08/062)
- Pacucci, F., Mesinger, A., & Haiman, Z. 2013, MNRAS, 435, L53, doi: [10.1093/mnrasl/slt093](https://doi.org/10.1093/mnrasl/slt093)
- Park, J., Gillet, N., Mesinger, A., & Greig, B. 2020, MNRAS, 491, 3891, doi: [10.1093/mnras/stz3278](https://doi.org/10.1093/mnras/stz3278)
- Rudakovskiy, A., Mesinger, A., Savchenko, D., & Gillet, N. 2021, MNRAS, 507, 3046, doi: [10.1093/mnras/stab2333](https://doi.org/10.1093/mnras/stab2333)
- Rudakovskiy, A., Savchenko, D., & Tsizh, M. 2020, MNRAS, 497, 3393, doi: [10.1093/mnras/staa2194](https://doi.org/10.1093/mnras/staa2194)
- Sabti, N., Muñoz, J. B., & Blas, D. 2022, PhRvD, 105, 043518, doi: [10.1103/PhysRevD.105.043518](https://doi.org/10.1103/PhysRevD.105.043518)
- Salpeter, E. E. 1955, ApJ, 121, 161, doi: [10.1086/145971](https://doi.org/10.1086/145971)
- Schultz, C., Oñorbe, J., Abazajian, K. N., & Bullock, J. S. 2014, MNRAS, 442, 1597, doi: [10.1093/mnras/stu976](https://doi.org/10.1093/mnras/stu976)
- Sheth, R. K., & Tormen, G. 2002, MNRAS, 329, 61, doi: [10.1046/j.1365-8711.2002.04950.x](https://doi.org/10.1046/j.1365-8711.2002.04950.x)
- Shevchuk, T., Kovetz, E. D., & Zitrin, A. 2023, arXiv e-prints, arXiv:2308.14640, doi: [10.48550/arXiv.2308.14640](https://doi.org/10.48550/arXiv.2308.14640)
- Spergel, D. N., & Steinhardt, P. J. 2000, PhRvL, 84, 3760, doi: [10.1103/PhysRevLett.84.3760](https://doi.org/10.1103/PhysRevLett.84.3760)
- Stücker, J., Angulo, R. E., Hahn, O., & White, S. D. M. 2022, MNRAS, 509, 1703, doi: [10.1093/mnras/stab3078](https://doi.org/10.1093/mnras/stab3078)
- Sun, G., & Furlanetto, S. R. 2016, MNRAS, 460, 417, doi: [10.1093/mnras/stw980](https://doi.org/10.1093/mnras/stw980)
- Viel, M., Becker, G. D., Bolton, J. S., & Haehnelt, M. G. 2013, PhRvD, 88, 043502, doi: [10.1103/PhysRevD.88.043502](https://doi.org/10.1103/PhysRevD.88.043502)
- Villasenor, B., Robertson, B., Madau, P., & Schneider, E. 2023, PhRvD, 108, 023502, doi: [10.1103/PhysRevD.108.023502](https://doi.org/10.1103/PhysRevD.108.023502)